Saline Water Desalination Using Direct Contact Membrane Distillation: A Theoretical and Experimental Investigation

Yasser Elhenawy, Kareem Fouad, Thokozani Majozi, Shereen M. S. Majozi, and M. Bassyouni

1 Introduction

The increase of various pollutants in freshwater sources to unprecedented proportions with the limitations of these sources portends many problems in the future. Therefore, all countries seek to find alternative sources of pure water through the

Y. Elhenawy · T. Majozi
School of Chemical and Metallurgical Engineering, University of the Witwatersrand, Johannesburg 2000, South Africa
e-mail: yasser.elhenawy@wits.ac.za

T. Majozi
e-mail: Thokozani.Majozi@wits.ac.za

Y. Elhenawy
Mechanical Power Engineering Department, Port-Said University, Port Said 42526, Egypt

Y. Elhenawy · M. Bassyouni (✉)
Center of Excellence in Membrane-Based Water Desalination Technology for Testing and Characterization (CEMTC), Port Said University, Port Said 42526, Egypt
e-mail: m.bassyouni@eng.psu.edu.eg

K. Fouad
Civil Engineering Department, Higher Future Institute of Engineering and Technology, El Mansoura, Egypt
e-mail: engkareem.s.civil@gmail.com

S. M. S. Majozi
Chemical Engineering Department, Egyptian Academy for Engineering and Advanced Technology Affiliated to Ministry of Military Production, Cairo 3066, Egypt
e-mail: shereenahmed@eaeat.edu.eg

M. Bassyouni
Department of Chemical Engineering, Faculty of Engineering, Port Said University, Port Said 42526, Egypt

East Port Said University of Technology, Saini, Port Said 45632, Egypt

application of many technological methods [1–5]. Clean water and sanitation are major Sustainable Development Goals (SDGs). Consequently, many scholars are interested in discovering multiple sources of freshwater [6]. Egypt has over 2,400 km of shoreline on the Red Sea and the Mediterranean Sea, respectively. Desalination is employed as a sustainable water supply for residential purposes in various regions of the country. Desalination is now being used along the Red Sea coast to provide enough household water to tourist communities and resorts. This is since the economic price of a water unit in these places is significant enough to cover the expense of desalination [7]. Many approaches are available for the seawater desalination process. To isolate a solvent or specific solutes, semi-permeable or phase change membranes are employed in industrial desalination systems. Desalination techniques may thus be divided into two broad types [8–11]. The first type is the thermal or phase-change process in which the raw water is boiled or heated. Minerals, salts, and contaminants are extremely dense to be carried away by the steam created by boiling and hence persist in the raw water. In this process, the vapor is condensed and cooled. As known, the main thermal desalination techniques are multiple effect distillation (MED), vapor compression (VC), and multi-stage flash distillation (MSF). The second type is the single-phase membrane procedure, the salt rejection occurs without excessive energy or phase transition. Electrodialysis and reverse osmosis (RO) are the two most common membrane procedures (ED). These systems are costly for small volumes of freshwater and cannot be employed in areas with few maintenance facilities [12–15]. Since these systems are well-established, they are considered energy-intensive and ultimately related to non-renewable energy supplies. Also, they are considered complex and have numerous operational issues. Alternative methods, including forward osmosis (FO), and membrane distillation (MD) has been studied because of their potential benefits (produced water quality, simplicity, energy consumption, competence to be joined with renewable energies including solar energy, etc.) [16–19].

Membrane distillation (MD) is a thermal separation method that uses a hydrophobic membrane to aid phase change, allowing only vapor to pass through the membrane wall. This technique has the potential to be employed for the desalination of brackish water or saltwater. Also, it is employed for the enhancement of important compounds [20–22]. Trans-membrane distillation, capillary distillation, pre-evaporation, osmotic distillation, membrane distillation, and other terminology are used in the field of MD to identify the process [23, 24]. The phenomena of membrane distillation derive from the process's resemblance to conventional distillation. MD and conventional distillation depend on the equilibrium of vapor–liquid as the core for salt rejection, and they involve the latent heat of vaporization being provided to induce the phase change [25, 26]. Polyvinylidenefluoride (PVDF), polypropylene (PP), and polytetrafluoroethylene (PTFE) are the mainly utilized resources for MD membranes [27]. The membranes used have porosities ranging from 0.06 to 0.95, pore sizes ranging from 0.2 to 1.0 m, and thicknesses ranging from 0.04 to 0.25 mm [28, 29]. Table 1 offers a list of these materials' surface energies and thermal conductivities.

Table 1 Materials employed in MD and their reported surface energy and thermal conductivity [30]

Membrane material	Surface energy ($\times 10^{-3}$ N/m)	Thermal conductivity (W m^{-1} K^{-1})
PTFE	9.13	0.26
PP	30.2	0.18
PVDF	30.5	0.20

From table, PTFE has oxidation resistance, decent thermal and chemical stability with supreme hydrophobicity. In contrast, it has a significant conductivity in which a superior heat loss will happen through PTFE membranes. On the other hand, PVDF shows respectable mechanical strength, thermal resistance, and hydrophobicity, and could simply be equipped into membranes with adaptable pore assemblies via various methods. In the case of PP, it shows well chemical and thermal resistance [30]. Recently, novel membrane components, including fluorinated copolymers and carbon nanotubes [31, 32], have been created to create MD membranes with high porosity and hydrophobicity, and strong mechanical strength.

The estimated flow of flat sheet membranes is ~20–30 m^{-2} h^{-1} at input hot temperatures of 60 °C and cold temperatures of 20 °C [28]. In all MD designs, the water flow typically upsurges with the consumed temperature [33]. Whereas the contrast in vapor pressure across the membrane drives membrane distillation. A rise in feed temperature causes an increase in vapor pressure in the feed solution channel, which raises the trans-membrane vapor pressure. A theoretical model for forecasting the behavior of membrane distillation was investigated by Burgoyne et al. [34]. Permeating fluxes have been discovered using the mass and heat transfer equations, and they have been supported by experiments. The primary research looked at the impact of flat-plate module design in laminar flow regimes. It was discovered that a 50% reduction in membrane area tended to result in a 66% increase in water flow. This could be caused by the rapid liquid velocity, which thins the boundary layer. The water flux tends to increase with larger main channels, which enhances flow distribution throughout the membrane.

In the several described MD setups, the impact of the support temperature on the water flow has been extensively investigated. In all MD designs, the water flow usually upsurges with the feed temperature [33]. Although the temperature polarization effect rises with feed temperature, numerous research claim that it is preferable to operate at high feed temperatures due to the high evaporation efficiency and complete heat transfer from the feed to the permeate/cooling side [28, 33, 35–37]. However, it must be noted that operating at temperatures over 90 °C may result in a decrease in membrane selectivity and serious scaling issues. The majority of research [38, 39] shows that the influence of the supply flow rate is to enhance the water flux. This is because the integration effect brought on by the boosted confusion through the feed channel has reduced the temperature and concentration polarisation influences. As a consequence of the turbulence, the temperature at the membrane surface

approaches the bulk input temperature. Because of the larger trans-membrane temperature decrease at higher temperatures, the influence of the flow rate on the production is excluding than half that of the influence of the input temperature [40]. In general, up to a certain point, the relationship between the feed flow rate and the trans-membrane flux is linear [40]. Chan et al. [41] tested the membrane distillation crystallization procedure. This investigation shows that the MD can function at high concentrations with fluxes up to 20 l/h m^2 at feed temperatures of 50 and 60 °C. Working at batch concentration, the flux steadily decreases as a result of concentration polarisation and vapor pressure suppression. Due to temperature polarization, which prevents salt saturation and scale deposition, the investigations revealed that the membrane wall temperature is ~5–10 °C lower than the bulk temperature. Based on the aforementioned studies, this paper applied a theoretical and experimental investigation to study the effect of a PTFE direct contact membrane sheet's geometric dimensions on the water flux.

2   Methods

This section presents details of the experimental and theoretical work of the flat sheet membrane distillation unit. The experimental equipment design and operational characteristics are described for the water desalination system.

2.1   *Experimental Setup Description*

Figure 1 depicts a schematic representation of the flat sheet DCMD technique for PTFE membrane materials. In the existing experiments, a flat sheet membrane with dimensions of 20 cm × 20 cm and an operative membrane area of 15 cm × 15 cm is employed. The permeate streams are depicted in blue in Figs. 1 and 2, whereas the warm streams are denoted in red. The membrane module and the electrical heater (1) are connected by the hot water pump (2), which moves the heated fluid between them (6). Via the top port aperture, the hot fluid is sent to the membrane module. Due to the related energy being lost to the vapor passing through the membrane, the hot feed temperature drops in the feed channel. The electrical heater (1) makes up for the temperature loss by raising the temperature of the hot stream to its starting point. The temperature of the feed fluctuates from 40 to 80 °C. Between the membrane module and the chiller (7), the cold water pump (8) circulates the cold water (6). Condensate from the vapor permeate raises the temperature of the cooled water as it passes through the permeate channel. The chilled stream is brought back to the original permeate temperature using the chiller function. The permeate temperature is managed by the chiller and is typically kept between 20 and 30 °C. Rotameters are used to measure the feed and permeate flow rates. Pressure transducers and thermocouples of type T are used, respectively to detect pressure and temperature.
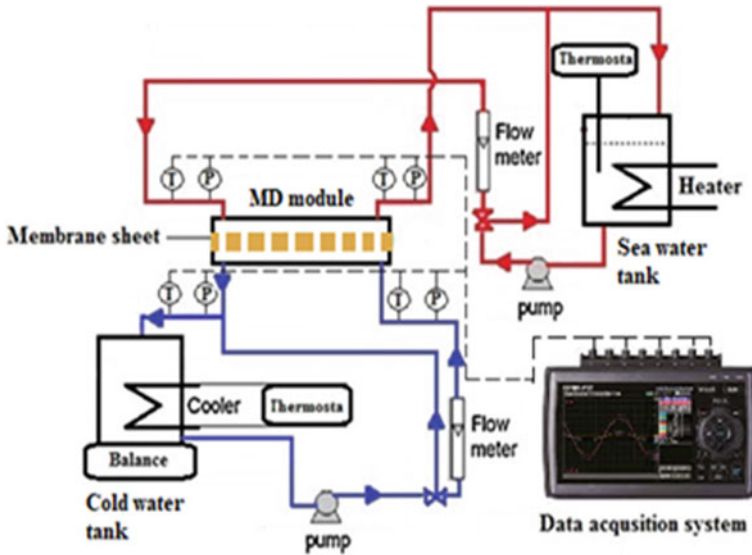
Fig. 1 A flow schematic of the DCMD unit

Using a weighing balance, the weight of the distillate is used to calculate the mass flow. The TDS meter model measures the brine and permeate concentrations. DATAQ Instruments (Graphtec Model: GL220 820APS, Graphtec) are used to record the data. NaCl with a salinity of 35 g/L is utilized as the feed solution in order to study the impact of feed salinity. The flow regime in the feed channel is laminar since the feed and permeate were set to the same flow rate and varied between 0.3 and 0.9 L/min (0.15 and 0.50 m/s).

The polypropylene non-woven layer utilized in experiments is laminated onto a membrane layer comprised of pure PTFE in the membrane flat sheet. The USA-based STERLITECH Company is where membranes are acquired. Table 2 lists the membrane's primary characteristics.

2.2 Heat and Mass Transfer of One-Dimension Model for DCMD

While the heat movement inside the MD unit is frequently described in three phases as illustrated in Fig. 3, water vapor transportation in membrane distillation may be a contemporaneous heat and mass transference process.

(I) The bulk input to the vapor–liquid membrane results in heat convection at the membrane exterior.
(II) Conductivity via the microporous membrane and evaporation.

Fig. 2 DCMD experimental unit: (1) heater supply basin, (2) supply pump, (3) filter, (4) rotameter, (5) thermocouple, (6) DCMD unit, (7) permeate tank (with chiller), (8) permeate pump, (9) electronic balance, (10) a pressure transducer, (11) DAQ scheme

**Table 2** Properties of the PTFE membrane sheet

Description	Specification
Pore size	0.45 μm
Thickness	127 μm
porosity	60–70%
Dimension	300 × 300 mm

(III) Heat convection, or the thermal physical phenomena of the permeate side, from the vapor/liquid boundary to the bulk, permeate at the membrane face [30].

It is assumed that the flux (J) depends on a variety of factors for a particular DCMD system, and a general connection may be expressed as

$$J = f\left(A, T_f, T_p, \dot{m}_f, \dot{m}_p, C_{membrane}, U\right) \tag{1}$$

Fig. 3 Mass and heat and transmission section of a parallel flow DCMD
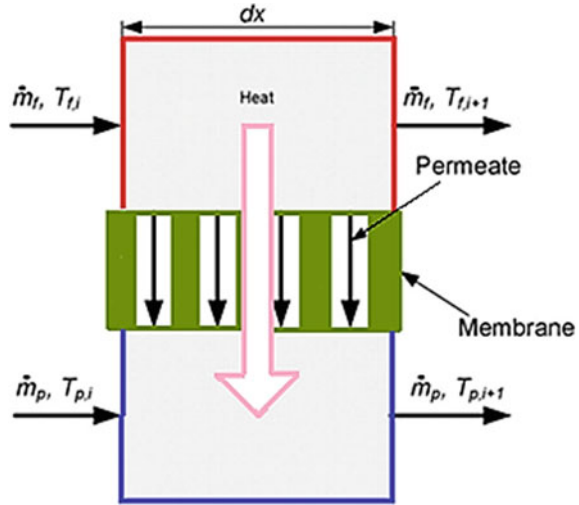
Here, $\dot{m}_p$ and $\dot{m}_f$ are the rates of mass flow for the cold face and feed side (hot flow).
To further simplify the model, the following presumptions were also made:

1. There is no heat loss through the unit wall.
2. According to R. G. Lunnon's discovery [41], the specific heat of condensation and evaporation does not alter among concentrations.
3. Across the membrane, no temperature descent perpendicular to the flow guidance, and C_{global} and U remain constant for a given membrane at a given flow rate.
4. Typically, below 3% of the total apparent thermal energy transported by the vapor is delivered to the cold face, it is possible to ignore the sensible heat carried by the permeate when balancing the heat transfer.

These presumptions allow us to express the flow as:

$$J = C_{global}\left(P_{Tf} - T\,P_{Tp}\right) \tag{2}$$

where C_{global} involves the processes of mass transport in the membrane and the boundary layer.

Figure 3 depicts a parallel flow DCMD heat and mass transfer element in a flat sheet unit. Change in thermal energy on the hot face in this element may be stated as follows:

$$C_{p,f}\dot{m}_f\left(T_{f,i+1} + T_{f,i}\right) = -\left(J\,H_{latent}\,dA + U\left(T_f - T_p\right)dA\right) \tag{3}$$

where $T_{f,i}$ and $T_{f,i+1}$ are temperatures at the ith and (i + 1) th points, and $C_{p,f}$ is the specific heat of feed.

$dA = Wdx$, where W is the width of the membrane, the relation among the stream displacement and temperature difference can be stated as,

$$dT_f = -\frac{W\left(J_i H_{latent} + U\left(T_{f,i} - T_{p,i}\right)\right)}{C_{p,f}\dot{m}_f}dx \tag{4}$$

As a result, the input temperature change after the feed stream passes through each element can be stated as follows:

$$\Delta T_{f,i} = -\frac{C_{global}\left[EXP\left(23.1964 - \frac{3816.44}{T_{f,i}+227.02}\right) - EXP\left(23.1964 - \frac{3816.44}{T_{p,i}+227.02}\right)\right]H_{latent} + U\left(T_{f,i} - T_{p,i}\right)}{C_{p,f}\dot{m}_f}W\Delta x \tag{5}$$

Because C_{global} and U are supposed to be constants, the temperature of the input stream at $(i + 1)$th can be computed by

$$T_{f,i+1} = T_{f,i} - \Delta T_{f,i} \tag{6}$$

The permeate temperature may be determined similarly by

$$T_{p,i+1} = T_{p,i} - \frac{\dot{m}_f}{\dot{m}_p}\Delta T_{f,i} \tag{7}$$

Thus, the flux at $(i + 1)$th can be revealed as:

$$J_{i+1} = C_{global}\left(P_{Tf,i+1} - P_{T,i+1}\right) \tag{8}$$

This allows for the calculation of the membrane's overall flux as

$$J = \frac{\sum_{i=0}^{N} J_i W \Delta x}{A} - \frac{\sum_{i=0}^{N} J_i \Delta x}{L} \tag{9}$$

The aforementioned equations can be computationally solved.

3   Results and Discussions

This section illustrates the influence of the DCMD operating parameters on the system's productivity. The influence of feed inlet temperature, membrane effective length, velocity, temperature difference, and feed velocity on the final flux.

3.1   Model Validation

Figure 4 shows the anticipated derived flux, which is the outcome of a parallel flow DCMD. The model was run with a constant velocity of 0.35 m/s (0.7 L/min) with various hot inlet temperatures (40–80) °C. Increasing feed inlet temperature
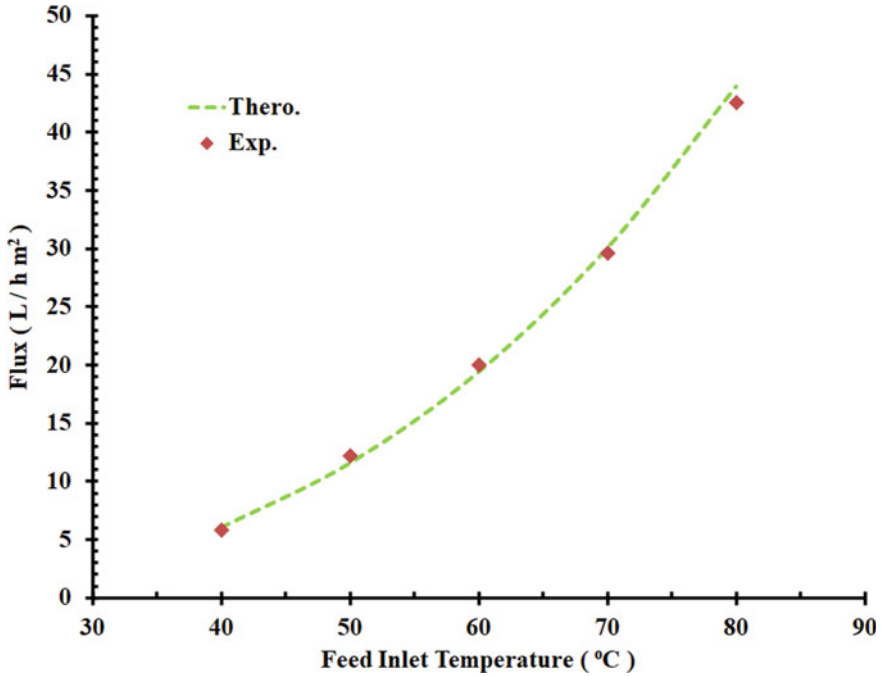
Fig. 4 Validation of experimental and theoretical results at different feed inlet temperatures

significantly boosts the output flux. This trend is the same as in a previous study [42]. Comparison between experimental and theoretical results shows that the simulation results well agree with the experimental outcomes and the maximum error is less than 1%, indicating that the proposed model is reliable and valid.

Figure 5 illustrates the comparison between experimental and theoretical results from parallel flow setups. Because a shorter membrane will result in a greater average temperature and differential through the membrane [43]. With a shorter retention period for mass and heat transfers, the membrane length influences the productivity of the membrane for certain stream velocities and intake temperatures. As a result, if the membrane size is not taken into account, it is inappropriate to assess the function of MD membranes by flux even when the inlet temperature and velocity are the same. Model validation shows that the maximum error is < 4% indicating that the proposed model is valid.

3.2 Temperature Distribution Along the Membrane Sheet

The temperature profiles predicted by parallel flow DCMD along the stream flow direction are shown in Fig. 6. Local temperatures on both faces of the membrane in
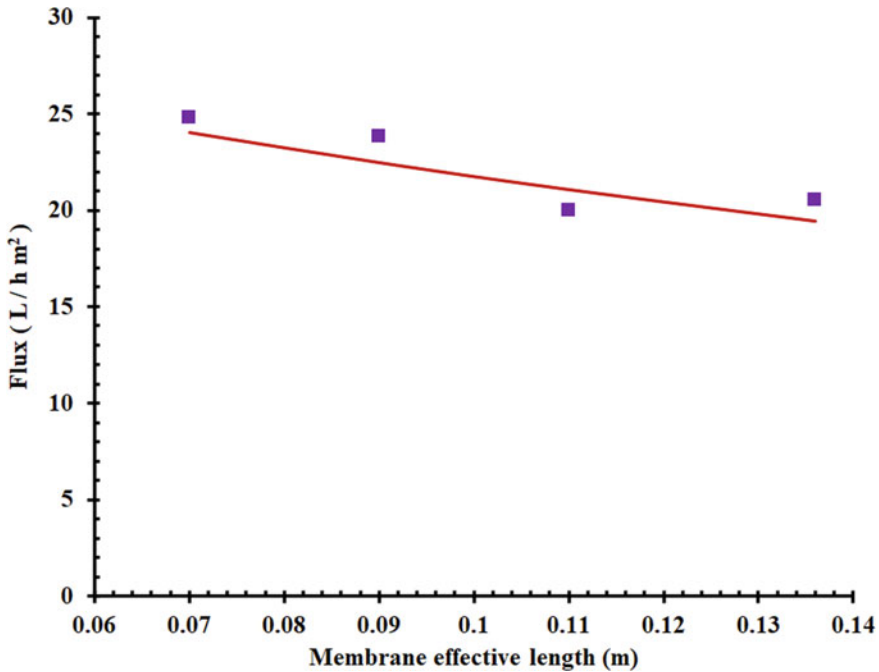
Fig. 5 Comparison between experimental and theoretical results for different membrane lengths

the parallel flow approach one another at points further from the entrance (origin). It is possible to predict that the flux of parallel flow mode would decrease laterally the feed low trend due to a smaller temperature variance based on the difference in the temperature profile [44].

3.3 Average Temperature Difference Across the Sides of the Membrane

Employing the computed heat and mass transfer coefficients from the created database was operated. Figure 7 illustrates the expected mean temperature difference across the membrane at various speeds. This chart showed that when the stream velocity decreased, the temperature differential enhanced. When the velocity increased from 0.2 to 0.45 m/s, the temperature difference decreased from 29 to 24 °C, which resulted in a temperature difference decrease of about 17%. This result is following a previous study [45].
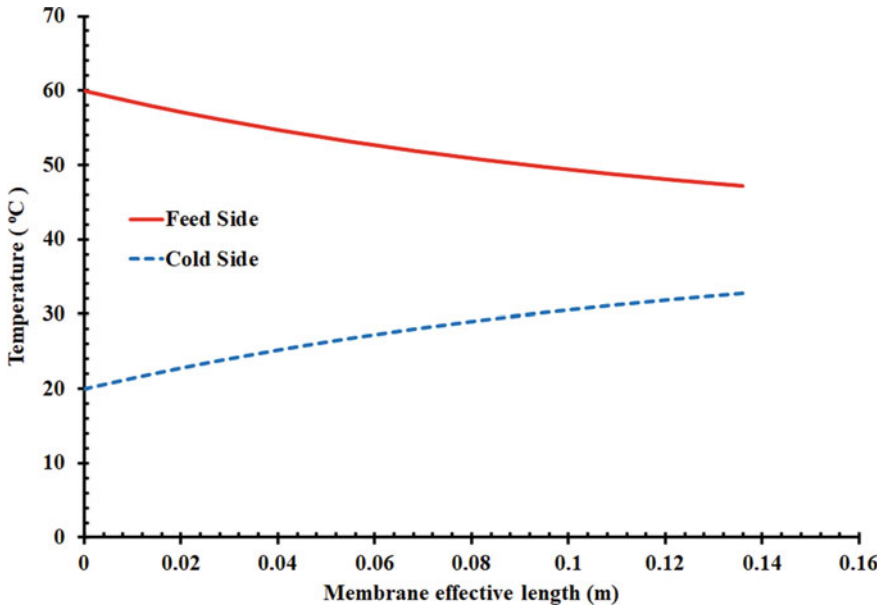
Fig. 6 Temperature distributions along the membrane sheet (supply velocity = 0.35 m/s, supply inlet temperature = 65 °C, cold inlet temperature = 20 °C)
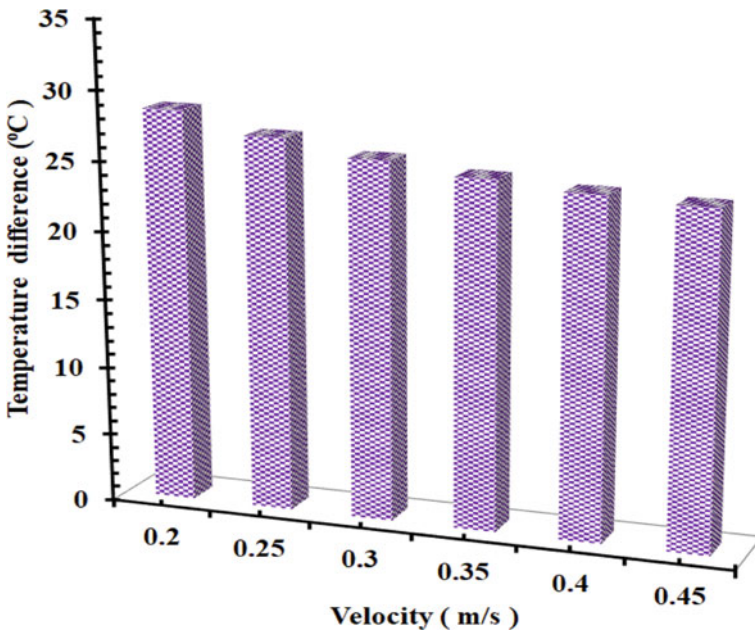

Fig. 7 Mean temperature differential across the membrane's sides at varying velocities (Membrane span = 0.145 m, supply inlet temperature = 65 °C, cold inlet temperature = 20 °C)
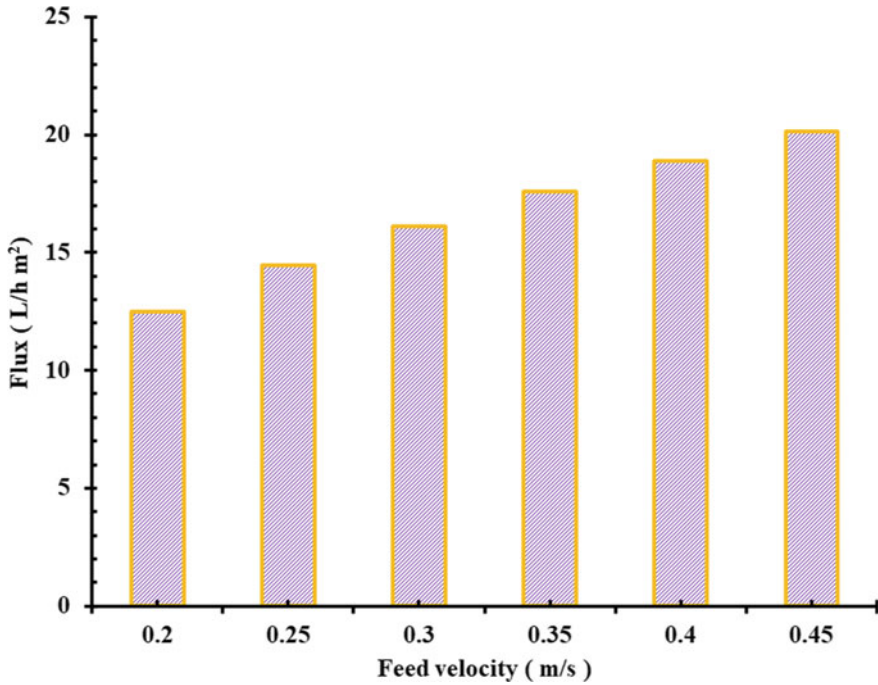
Fig. 8 Flux at different velocities (membrane length = 0.145 m, feed inlet temperature = 65 °C, cold inlet temperature = 20 °C)

3.4 Influence of Feed Velocity on Flux

Figure 8 illustrates the influence of feed velocity on the final flux. Increasing the feed velocity showed a significant boost in water productivity. This is due to the reduction in the residence time which is influenced by the boosted feed velocity [32]. The maximum flux reached about 20 L/h m^2 at a feed velocity of 0.45 m/s.

3.5 Influence of Membrane Different Effective Lengths on Flux

Figure 9 depicts the flow changes along the membrane's length at various speeds. When the velocity rose by around 0.065 m/s, the overall flux differential decreased from 4.6 to 2.3 L m^{-2} h^{-1}. The trustworthiness of the model predictions is further supported by the previously documented tendency of permeate flux with boosting feed flow rates. The figures also demonstrate that when longer membranes are utilized, the difference in flux at different speeds decreases. Hence, when larger
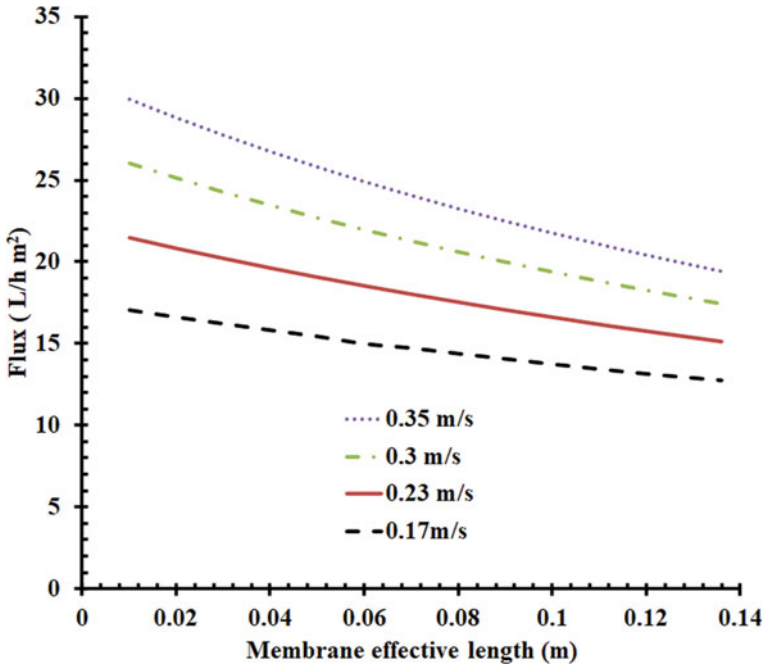
Fig. 9 Flux variance of parallel flow DCMD in the direction of the flow at various velocities (inlet feed temperature = 65 °C, inlet cold temperature = 20 °C)

membrane dimensions are used, the influence of feed velocity on flow will diminish [28].

4   Conclusions

This paper investigated experimentally and theoretically the desalination of saline water using direct contact membrane distillation. A polytetrafluoroethylene (PTFE) membrane was employed with a pore size of 0.45 μm and supported by a scrim layer in a desalination unit. The experimental results showed that the average overall mass and heat transfer coefficients slightly variate with changes in certain factors. These factors are the temperature difference between (40–80 °C) and membrane span variance, which serve as a basis for the simple model's validity. The basic model may be utilized to forecast productivity at various temperatures and membrane spans. Furthermore, the module flow channel structure's properties, such as the existence of a turbulence promoter (spacer) or the size of the flow channel cross-section, will have a substantial impact on the established boundary layer conditions. As a result, changes in these flow channel characteristics will invalidate the previous database at the same stream velocity. The model's predictions demonstrated that when the flow

rates on both sides are the same, the temperature profiles on the hot and cold sides approach one another. Also, MD flux is influenced by membrane length, therefore it is advised to employ a short, broad membrane for high production requests adequately extended, slim membrane scheme. The simulation findings demonstrated that for longer membranes, the supply velocity will have a lower impact on flow. Finally, the comparison between experimental and theoretical results shows that the simulation results well agree with the experimental outcomes indicating that the proposed model is reliable and valid.

5   Recommendations

Polytetrafluoroethylene (PTFE) membranes have proven to be highly efficient in operating as desalination membranes. The proposed simulation model has proven the predictability of desalination results by (PTFE) membranes. This model could be used for other types of membranes to get the best types and conditions. Also, the validation error could be reduced by improving the simulation inputs or by trying artificial intelligence methods.

References

1. Fouad K, Gar Alalm M, Bassyouni M, Saleh MY (2020) A novel photocatalytic reactor for the extended reuse of W-TiO$_2$ in the degradation of sulfamethazine. Chemosphere 257:127270. https://doi.org/10.1016/j.chemosphere.2020.127270
2. Fouad K, Bassyouni M, Alalm MG, Saleh MY (2021) Recent developments in recalcitrant organic pollutants degradation using immobilized photocatalysts. Appl Phys A Mater Sci Process 127:612. https://doi.org/10.1007/s00339-021-04724-1
3. Fouad K, Bassyouni M, Alalm MG, Saleh MY (2021) The treatment of wastewater containing pharmaceuticals. J Environ Treat Tech 9:499–504. https://doi.org/10.47277/JETT/9(2)504
4. Fouad K, Gar Alalm M, Bassyouni M, Saleh MY (2021) Optimization of catalytic wet peroxide oxidation of carbofuran by Ti-LaFeO$_3$ dual photocatalyst. Environ Technol Innov 23:101778. https://doi.org/10.1016/j.eti.2021.101778
5. El-Gamal H, Radwan K, Fouad K (2020) Floatation of activated sludge by nascent prepared carbon dioxide (Dept. C (Public)). Bull Fac Eng Mansoura Univ 40:21–29. https://doi.org/10.21608/bfemu.2020.101236
6. Elhenawy Y, Fouad K, Bassyouni M, Majozi T (2023) Design and performance a novel hybrid membrane distillation/humidification–dehumidification system. Energy Convers Manag 286:117039. https://doi.org/10.1016/j.enconman.2023.117039
7. Elsaie Y, Ismail S, Soussa H, Gado M, Balah A (2023) Water desalination in Egypt; literature review and assessment. Ain Shams Eng J 14:101998. https://doi.org/10.1016/j.asej.2022.101998

8. Elhenawy Y, Moustafa GH, Abdel-Hamid SMS, Bassyouni M, Elsakka MM (2022) Experimental investigation of two novel arrangements of air gap membrane distillation module with heat recovery. Energy Rep 8:8563–8573. https://doi.org/10.1016/j.egyr.2022.06.068

9. Mansi AE, El-Marsafy SM, Elhenawy Y, Bassyouni M (2022) Assessing the potential and limitations of membrane-based technologies for the treatment of oilfield produced water. Alexandria Eng J 68:787–815. https://doi.org/10.1016/j.aej.2022.12.013

10. Elhenawy Y, Moustafa GH, Mahmoud A, Mansi AE, Majozi T (2022) Performance enhancement of a hybrid multi effect evaporation/membrane distillation system driven by solar energy for desalination. J Environ Chem Eng 10:108855. https://doi.org/10.1016/j.jece.2022.108855

11. Zakaria M, Sharaky AM, Al-Sherbini AS, Bassyouni M, Rezakazemi M, Elhenawy Y (2022) Water desalination using solar thermal collectors enhanced by nanofluids. Chem Eng Technol 45:15–25. https://doi.org/10.1002/ceat.202100339

12. Alhathal Alanezi A, Bassyouni M, Abdel-Hamid SMS, Ahmed HS, Abdel-Aziz MH, Zoromba MS, Elhenawy Y (2021) Theoretical investigation of vapor transport mechanism using tubular membrane distillation module. Membranes (Basel). https://doi.org/10.3390/membranes11080560

13. Mabrouk A, Elhenawy Y, Mostafa G, Shatat M, El-Ghandour M (2016) Experimental evaluation of novel hybrid multi effect distillation–membrane distillation (MED-MD) driven by solar energy. Desalin Environ Clean Water Energy 2016, 22–26

14. Alanezi AA, Safaei MR, Goodarzi M, Elhenawy Y (2020) The effect of inclination angle and Reynolds number on the performance of a direct contact membrane distillation (DCMD) process. Energies 13(11):2824

15. Elhady S, Bassyouni M, Mansour RA, Elzahar MH, Abdel-Hamid S, Elhenawy Y, Saleh MY (2020) Oily wastewater treatment using polyamide thin film composite membrane technology. Membranes (Basel) 10:84. https://doi.org/10.3390/membranes10050084

16. Elhenawy Y, Fouad Y, Marouani H, Bassyouni M (2021) Performance analysis of reinforced epoxy functionalized carbon nanotubes composites for vertical axis wind turbine blade. Polymers (Basel) 13:1–16. https://doi.org/10.3390/polym13030422

17. Elsakka MM, Ingham DB, Ma L, Pourkashanian M, Moustafa GH, Elhenawy Y (2022) Response surface optimisation of vertical axis wind turbine at low wind speeds. Energy Rep 8:10868–10880. https://doi.org/10.1016/j.egyr.2022.08.222

18. Elhenawy Y, Hafez G, Abdel-Hamid S, Elbany M (2020) Prediction and assessment of automated lifting system performance for multi-storey parking lots powered by solar energy. J Clean Prod 266:121859. https://doi.org/10.1016/j.jclepro.2020.121859

19. Elbany M, Elhenawy Y (2021) Analyzing the ultimate impact of COVID-19 in Africa. Case Stud Transp Policy 9:796–804. https://doi.org/10.1016/j.cstp.2021.03.016

20. Marni Sandid A, Bassyouni M, Nehari D, Elhenawy Y (2021) Experimental and simulation study of multichannel air gap membrane distillation process with two types of solar collectors. Energy Convers Manag 243:114431. https://doi.org/10.1016/j.enconman.2021.114431

21. Elminshawy NAS, Gadalla MA, Bassyouni M, El-Nahhas K, Elminshawy A, Elhenawy Y (2020) A novel concentrated photovoltaic-driven membrane distillation hybrid system for the simultaneous production of electricity and potable water. Renew Energy 162:802–817. https://doi.org/10.1016/j.renene.2020.08.041

22. Elrasheedy A, Rabie M, El Shazly AH, Bassyouni M, El-Moneim AA, El Kady MF (2021) Investigation of different membrane porosities on the permeate flux of direct contact membrane distillation. Key Eng Mater Trans Tech Publ 889:85–90

23. Elrasheedy A, Rabie M, El-Shazly A, Bassyouni M, Abdel-Hamid SMS, El Kady MF (2021) Numerical investigation of fabricated MWCNTs/polystyrene nanofibrous membrane for DCMD. Polymers (Basel) 13:160. https://doi.org/10.3390/polym13010160

24. Bassyouni M, Abdel-Aziz MH, Zoromba MS, Abdel-Hamid SMS, Drioli E (2019) A review of polymeric nanocomposite membranes for water purification. J Ind Eng Chem 73:19–46. https://doi.org/10.1016/j.jiec.2019.01.045

25. Maddah HA, Alzhrani AS, Almalki AM, Bassyouni M, Abdel-Aziz MH, Zoromba M, Shihon MA (2017) Determination of the treatment efficiency of different commercial membrane modules for the treatment of groundwater. J Mater Environ Sci 8:2006–2012

26. Soliman MF, Abdel-Aziz MH, Bamaga OA, Gzara L, Al-Sharif SF, Bassyouni M, Rehan ZA, Drioli E, Albeirutty M, Ahmed I, Ali I, Bake H (2017) Performance evaluation of blended PVDF membranes for desalination of seawater RO brine using direct contact membrane distillation. Desalin Water Treat 63:6–14. https://doi.org/10.5004/dwt.2017.20175

27. Jiao B, Cassano A, Drioli E (2004) Recent advances on membrane processes for the concentration of fruit juices: a review. J Food Eng 63:303–324. https://doi.org/10.1016/j.jfoodeng.2003.08.003

28. Alklaibi AM, Lior N (2005) Membrane-distillation desalination: status and potential. Desalination 171:111–131. https://doi.org/10.1016/j.desal.2004.03.024

29. Zhang J, Dow N, Duke M, Ostarcevic E, De LJ, Gray S (2010) Identification of material and physical features of membrane distillation membranes for high performance desalination. J Memb Sci 349:295–303. https://doi.org/10.1016/j.memsci.2009.11.056

30. Curcio E, Drioli E (2005) Membrane distillation and related operations—a review. Sep Purif Rev 34:35–86

31. Dumee LF, Sears K, Schütz J, Finn N, Huynh C, Hawkins S, Duke M, Gray S (2010) Characterization and evaluation of carbon nanotube Bucky-Paper membranes for direct contact membrane distillation. J Memb Sci 351:36–43. https://doi.org/10.1016/j.memsci.2010.01.025

32. Zhang J, De LJ, Duke M, Xie Z, Gray S (2010) Performance of asymmetric hollow fibre membranes in membrane distillation under various configurations and vacuum enhancement. J Memb Sci 362:517–528. https://doi.org/10.1016/j.memsci.2010.07.004

33. El-Bourawi MS, Ding Z, Ma R, Khayet M (2006) A framework for better understanding membrane distillation separation process. J Memb Sci 285:4–29. https://doi.org/10.1016/j.memsci.2006.08.002

34. Burgoyne A, Vahdati MM, Priestman GH (1995) Investigation of flux in flat-plate modules for membrane distillation. Dev Chem Eng Miner Process 3:161–175. https://doi.org/10.1002/apj.5500030305

35. Izquierdo-Gil MA, García-Payo MC, Fernández-Pineda C (1999) Air gap membrane distillation of sucrose aqueous solutions. J Memb Sci 155:291–307. https://doi.org/10.1016/S0376-7388(98)00323-8

36. Ali A, Macedonio F, Drioli E, Aljlil S, Alharbi OA (2013) Experimental and theoretical evaluation of temperature polarization phenomenon in direct contact membrane distillation. Chem Eng Res Des 91:1966–1977. https://doi.org/10.1016/j.cherd.2013.06.030

37. Shirazi MMA, Kargari A, Tabatabaei M (2014) Evaluation of commercial PTFE membranes in desalination by direct contact membrane distillation. Chem Eng Process Process Intensif 76:16–25. https://doi.org/10.1016/j.cep.2013.11.010

38. Banat FA, Simandl J (1994) Theoretical and experimental study in membrane distillation. Desalination 95:39–52. https://doi.org/10.1016/0011-9164(94)00005-0

39. Bin AM, Wahab RA, Salam MA, Gzara L, Moujdin IA (2023) Desalination technologies, membrane distillation, and electrospinning, an overview. Heliyon 9:e12810. https://doi.org/10.1016/j.heliyon.2023.e12810

40. Lawson KW, Lloyd DR (1997) Membrane distillation. J Memb Sci 124:1–25. https://doi.org/10.1016/S0376-7388(96)00236-0

41. Chan MT, Fane AG, Matheickal JT, Sheikholeslami R (2005) Membrane distillation crystallization of concentrated salts—flux and crystal formation. J Memb Sci 257:144–155. https://doi.org/10.1016/J.MEMSCI.2004.09.051

42. Francis L, Ghaffour N, Alsaadi AA, Amy GL (2013) Material gap membrane distillation: a new design for water vapor flux enhancement. J Memb Sci 448:240–247. https://doi.org/10.1016/j.memsci.2013.08.013

43. Li G, Liu J, Zhang F, Wang J (2022) Heat and moisture transfer and dimension optimization of cross-flow hollow fiber membrane contactor for membrane distillation desalination. Sep Purif Technol 297:121576. https://doi.org/10.1016/j.seppur.2022.121576

44. Ghosh R, Madadkar P, Wu Q (2016) On the workings of laterally-fed membrane chromatography. J Memb Sci 516:26–32. https://doi.org/10.1016/j.memsci.2016.05.064
45. Hahne E, Chen Y (1998) Numerical study of flow and heat transfer characteristics in hot water stores. Sol Energy 64:9–18. https://doi.org/10.1016/S0038-092X(98)00051-6